Supporting Information

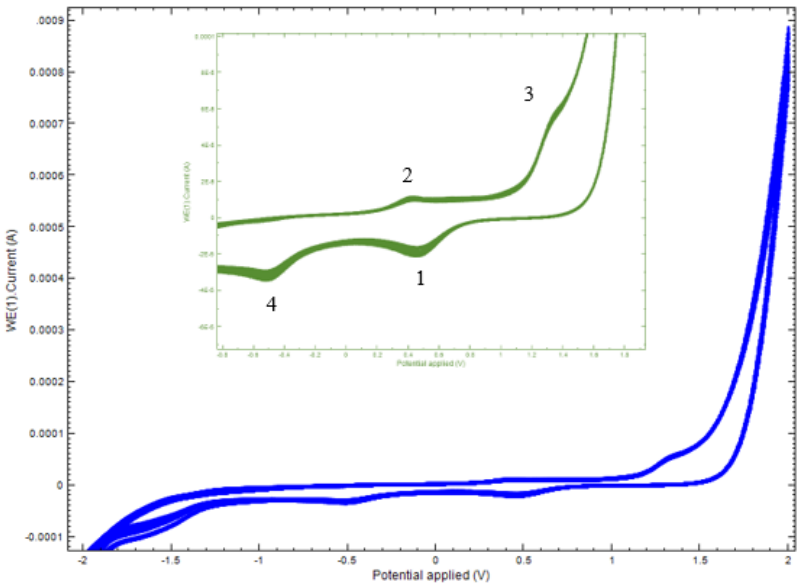

Figure S1. CV's of electropolymerization of *β*-CD on the surface of the GCE in the presence of 6 mM of *β*-CD dissolved in 0.05M PBS (pH=4) at 0.07 $V.s^{-1}$ with 40 number of cycles**.**

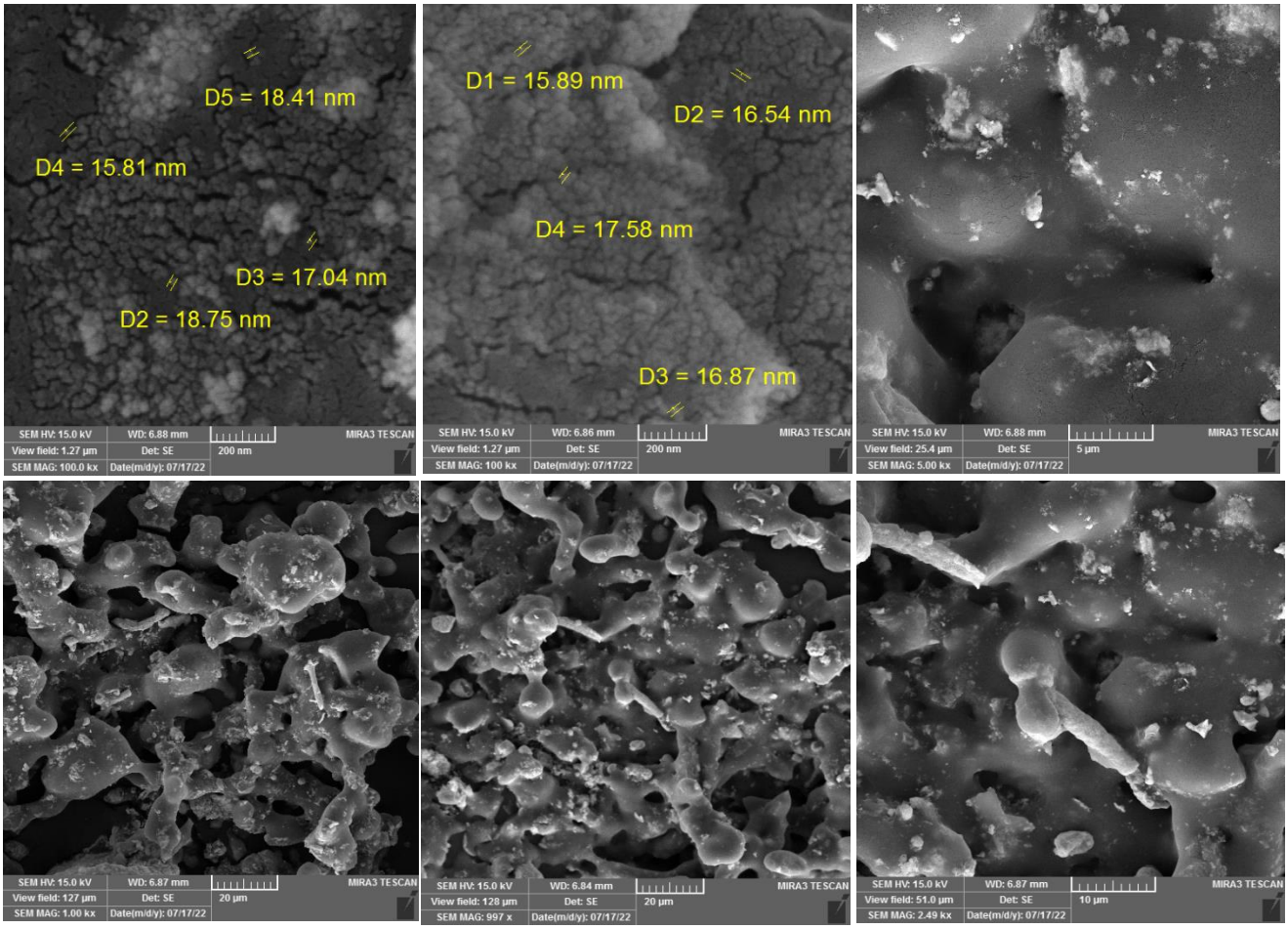

Elt	Line	Int	K	W%	A%
C	Ka	153.6	0.1385	23.50	37.47
O	Ka	545.8	0.2826	35.10	42.01
Na	Ka	889.2	0.2177	17.20	14.33
Cl	Ka	458.4	0.1622	8.68	4.69
Au	La	7.3	0.1990	15.51	1.51

Figure S2: FE-SEM illustrations of AuNPs-DDT in different magnification along with EDS.

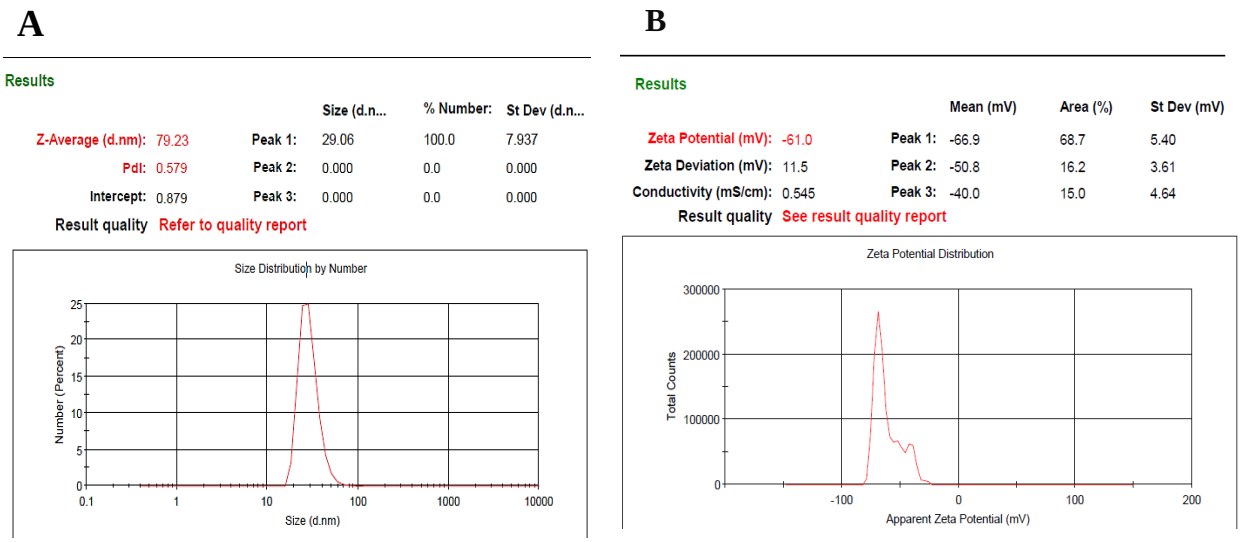

Figure *S3.A)* *DLS diagram of AuNPs-DDT.* ***B)*** *Zeta-Potential of AuNPs-DDT.*

A)

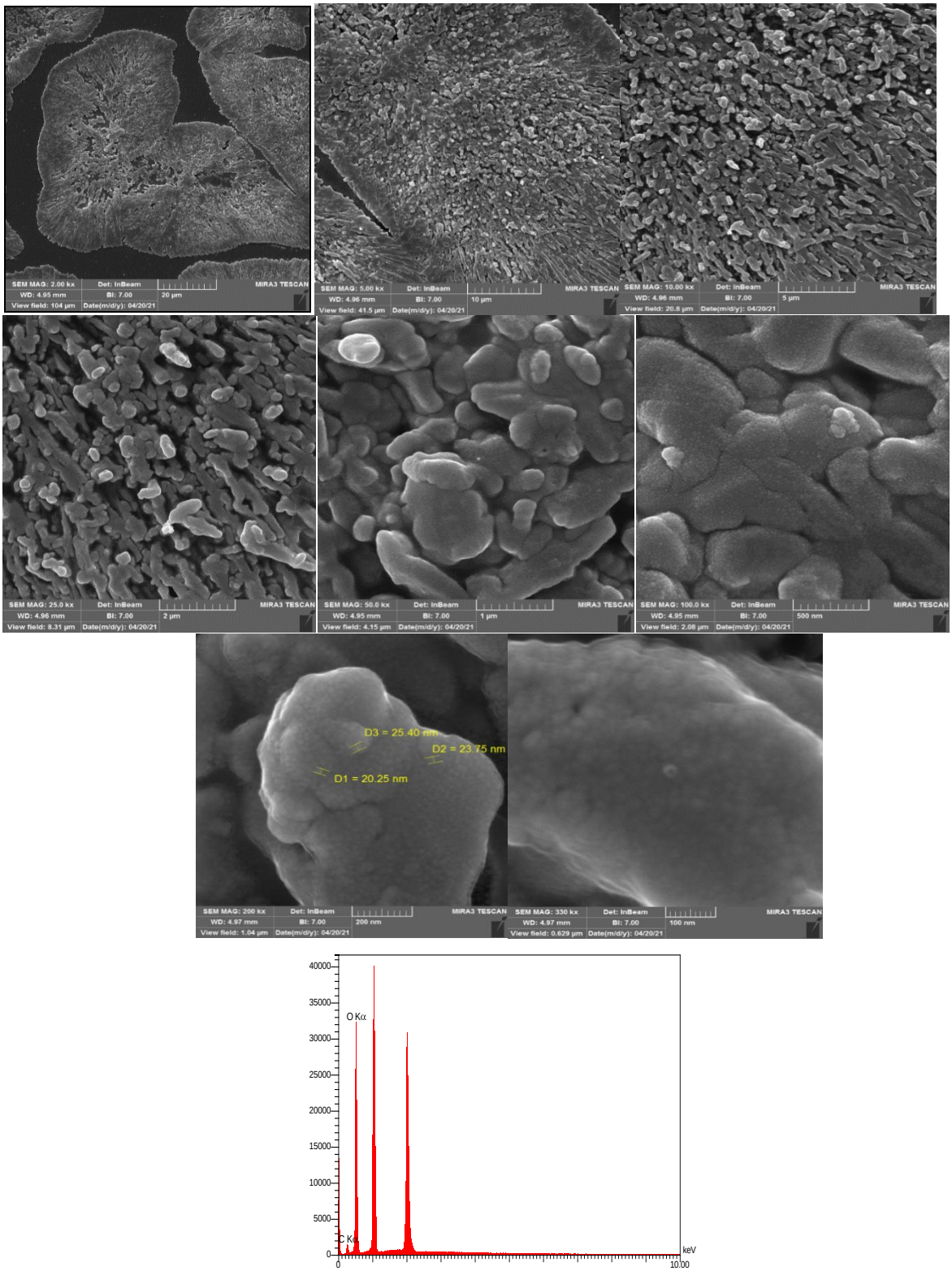
SEM MAG: 2.00 kx
Det: InBeam
WD: 4.95 mm
BI: 7.00
20 µm
View field: 104 µm
Date(m/d/y): 04/20/21
MIRA3 TESCAN
SEM MAG: 5.00 kx
WD: 4.96 mm
10 µm
View field: 41.5 µm
SEM MAG: 10.00 kx
WD: 4.96 mm
5 µm
View field: 20.8 µm
SEM MAG: 25.0 kx
WD: 4.96 mm
2 µm
View field: 8.31 µm
SEM MAG: 50.0 kx
WD: 4.95 mm
1 µm
View field: 4.15 µm
SEM MAG: 100.0 kx
WD: 4.95 mm
500 nm
View field: 2.08 µm
D3 = 25.40 nm
D2 = 23.75 nm
D1 = 20.25 nm
SEM MAG: 200 kx
WD: 4.97 mm
200 nm
View field: 1.04 µm
SEM MAG: 330 kx
WD: 4.97 mm
100 nm
View field: 0.629 µm
O Kα
C Kα
keV
40000
35000
30000
25000
20000
15000
10000
5000
0
0
10.00

B.

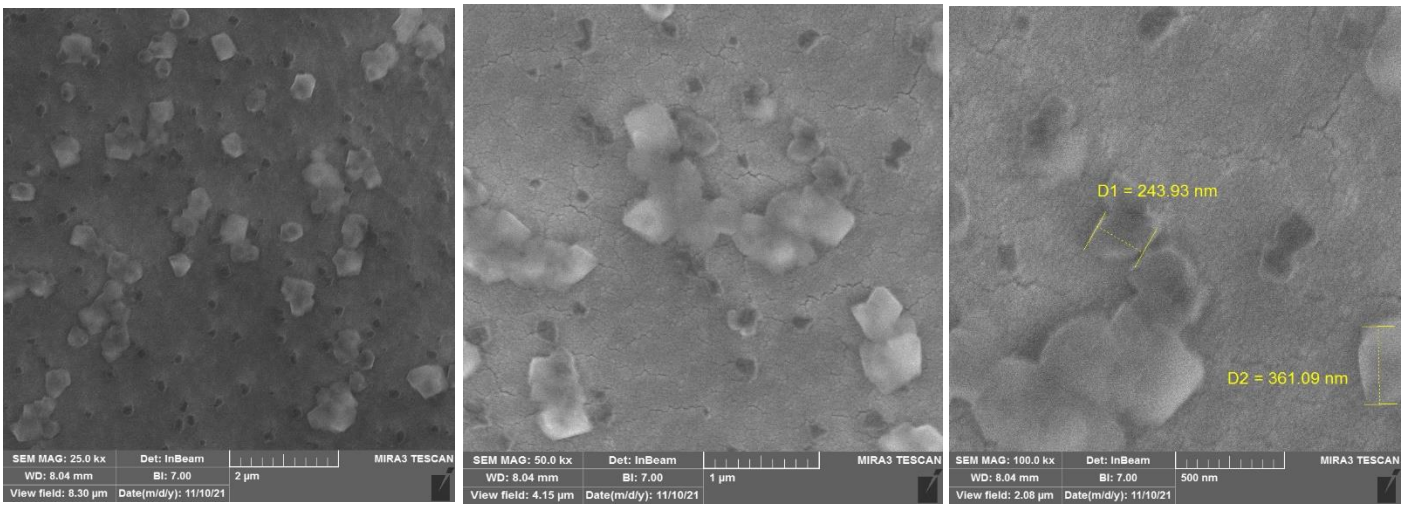
SEM MAG: 25.0 kx
Det: InBeam
WD: 8.04 mm
BI: 7.00
View field: 8.30 µm
Date(m/d/y): 11/10/21
2 µm
MIRA3 TESCAN
SEM MAG: 50.0 kx
Det: InBeam
WD: 8.04 mm
BI: 7.00
View field: 4.15 µm
Date(m/d/y): 11/10/21
1 µm
MIRA3 TESCAN
D1 = 243.93 nm
D2 = 361.09 nm
SEM MAG: 100.0 kx
Det: InBeam
WD: 8.04 mm
BI: 7.00
View field: 2.08 µm
Date(m/d/y): 11/10/21
500 nm
MIRA3 TESCAN

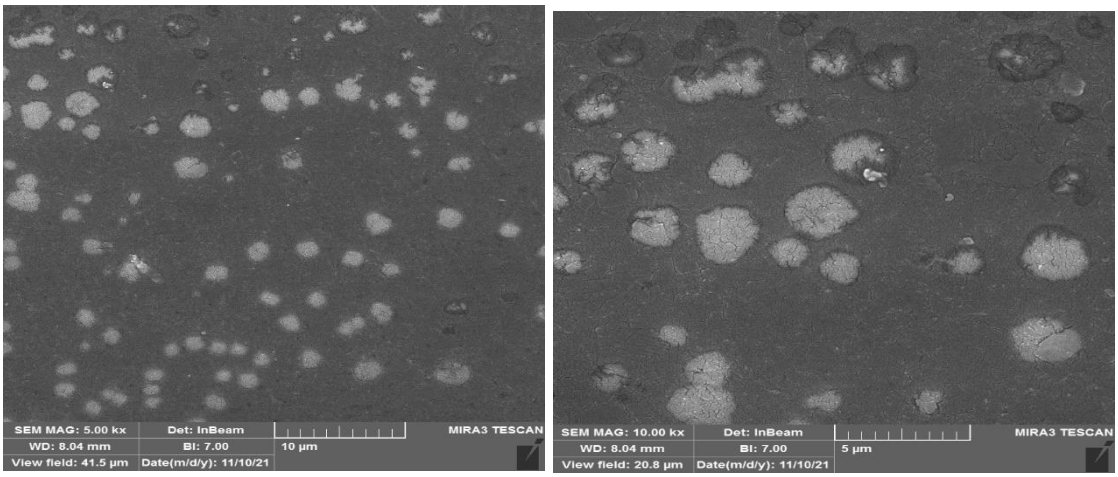
SEM MAG: 5.00 kx
Det: InBeam
WD: 8.04 mm
BI: 7.00
View field: 41.5 µm
Date(m/d/y): 11/10/21
10 µm
MIRA3 TESCAN
SEM MAG: 10.00 kx
Det: InBeam
WD: 8.04 mm
BI: 7.00
View field: 20.8 µm
Date(m/d/y): 11/10/21
5 µm
MIRA3 TESCAN

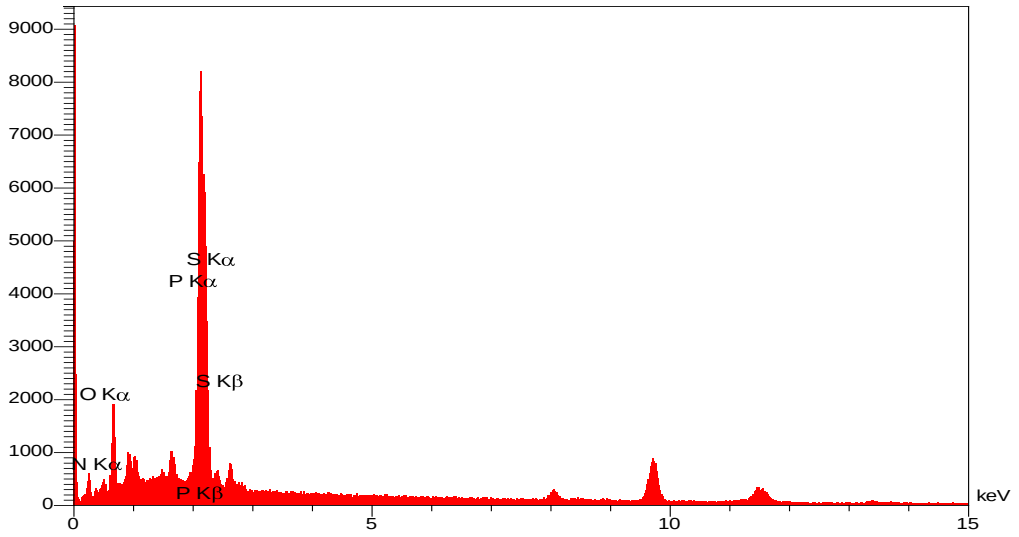
9000
8000
7000
6000
5000
4000
3000
2000
1000
0
S Kα
P Kα
S Kβ
O Kα
N Kα
P Kβ
0
5
10
15
keV

C.

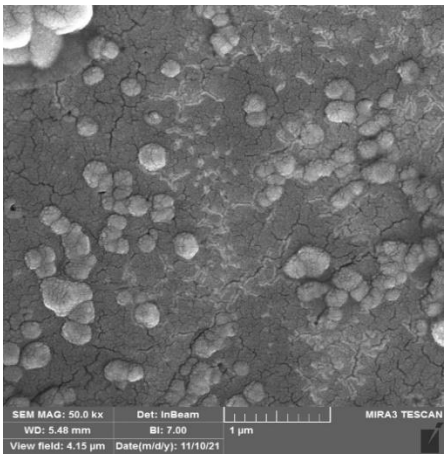
SEM MAG: 50.0 kx
Det: InBeam
WD: 5.48 mm
BI: 7.00
1 µm
View field: 4.15 µm
Date(m/d/y): 11/10/21
MIRA3 TESCAN

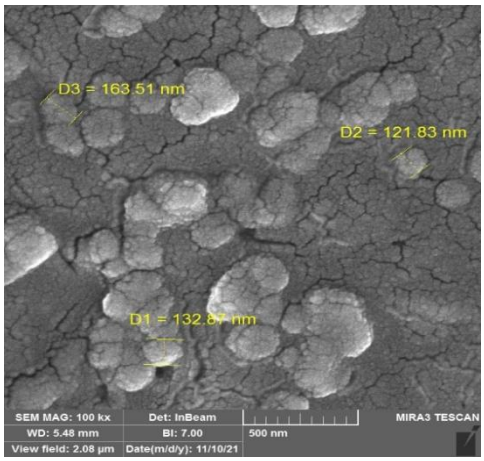
D3 = 163.51 nm
D2 = 121.83 nm
D1 = 132.87 nm
SEM MAG: 100 kx
Det: InBeam
WD: 5.48 mm
BI: 7.00
500 nm
View field: 2.08 µm
Date(m/d/y): 11/10/21
MIRA3 TESCAN

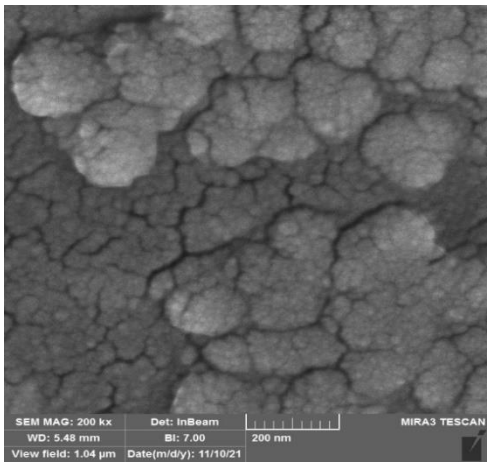
SEM MAG: 200 kx
Det: InBeam
WD: 5.48 mm
BI: 7.00
200 nm
View field: 1.04 µm
Date(m/d/y): 11/10/21
MIRA3 TESCAN

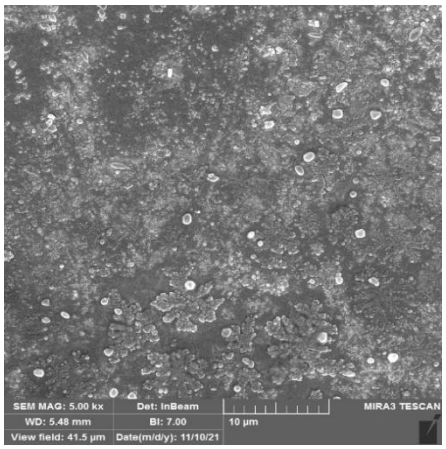
SEM MAG: 5.00 kx
Det: InBeam
WD: 5.48 mm
BI: 7.00
10 µm
View field: 41.5 µm
Date(m/d/y): 11/10/21
MIRA3 TESCAN

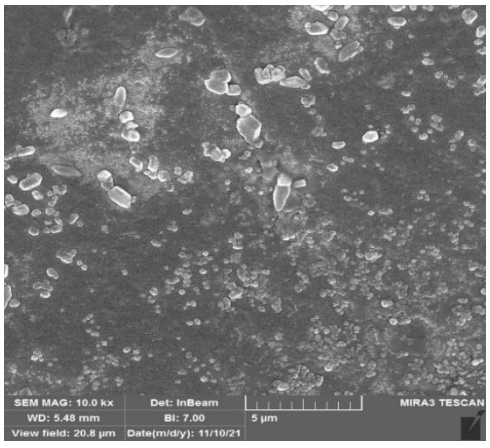
SEM MAG: 10.0 kx
Det: InBeam
WD: 5.48 mm
BI: 7.00
5 µm
View field: 20.8 µm
Date(m/d/y): 11/10/21
MIRA3 TESCAN

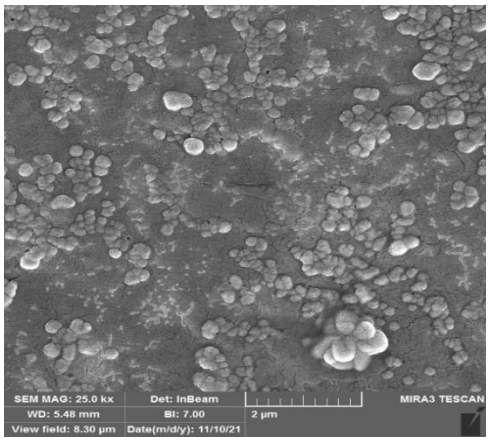
SEM MAG: 25.0 kx
Det: InBeam
WD: 5.48 mm
BI: 7.00
2 µm
View field: 8.30 µm
Date(m/d/y): 11/10/21
MIRA3 TESCAN

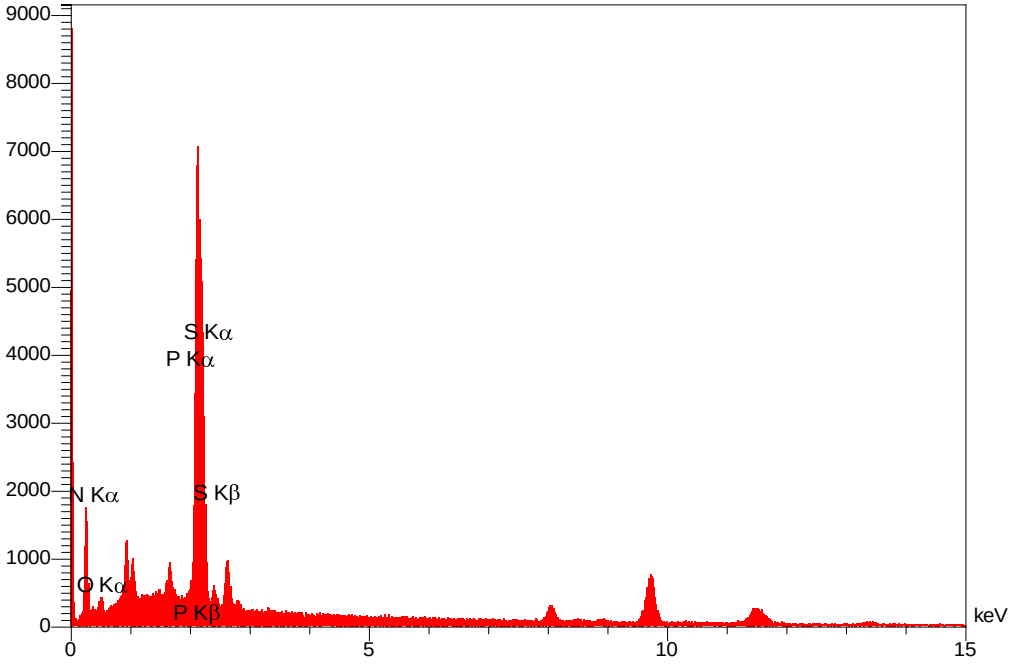
9000
8000
7000
6000
5000
4000
3000
2000
1000
0
S Kα
P Kα
N Kα
S Kβ
O Kα
P Kβ
0
5
10
15
keV

D.

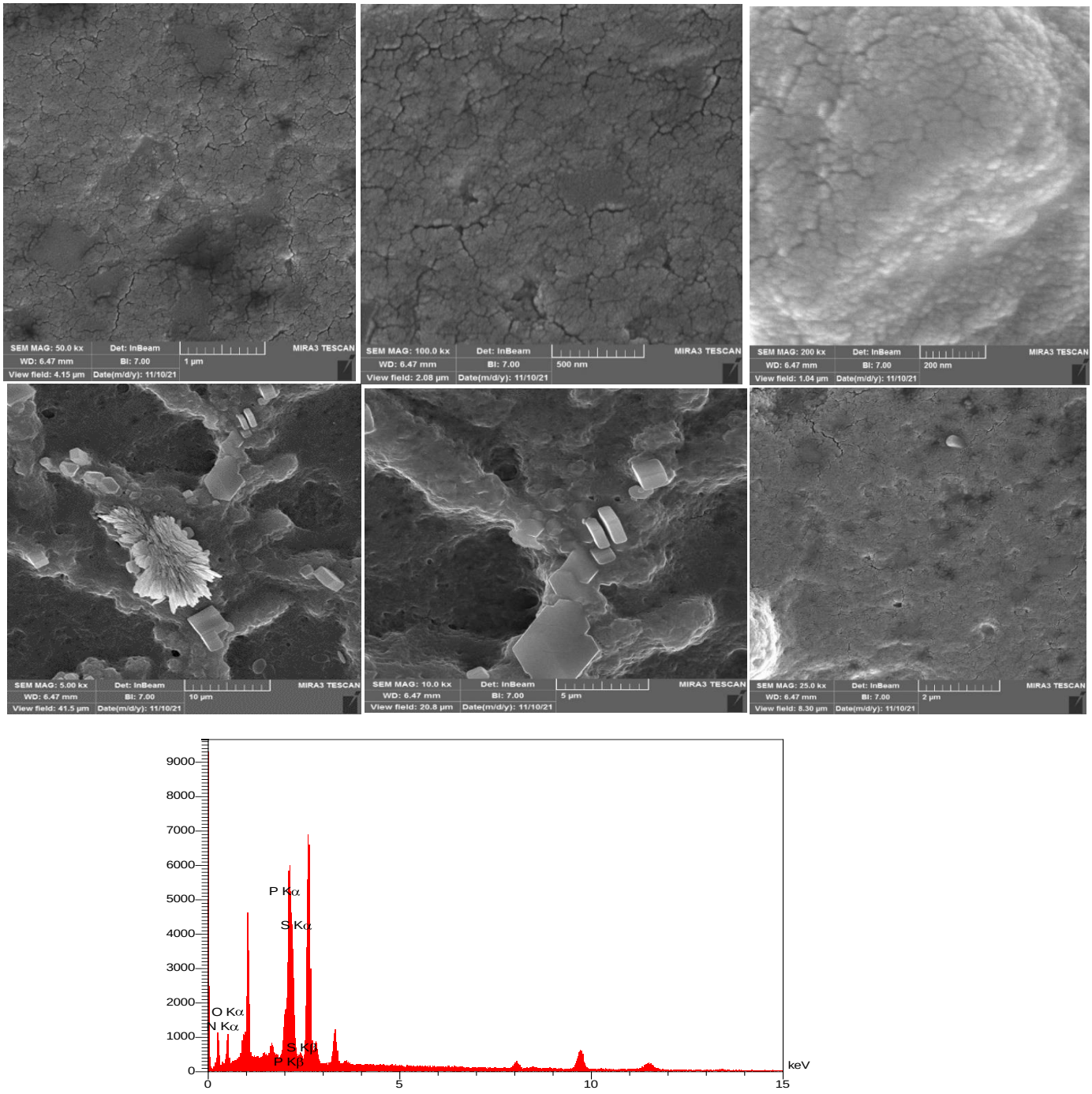

Figure S4. A: FE-SEM illustrations of P*β*-CD)-GCE in different magnification along with EDS. **B:** FE-SEM illustrations of P(*β*-CD)-Ab1-GCE in different magnification along with EDS. **C:** FE-SEM illustrations of P(*β*-CD) -Ab1- BSA -2-AG GCE in different magnification along with EDS. **D:** FE-SEM illustrations of P(β-CD) -Ab1- BSA -2-AG- Ab2-HRP/AuNPs/TB/GLU GCE in different magnification along with EDS.

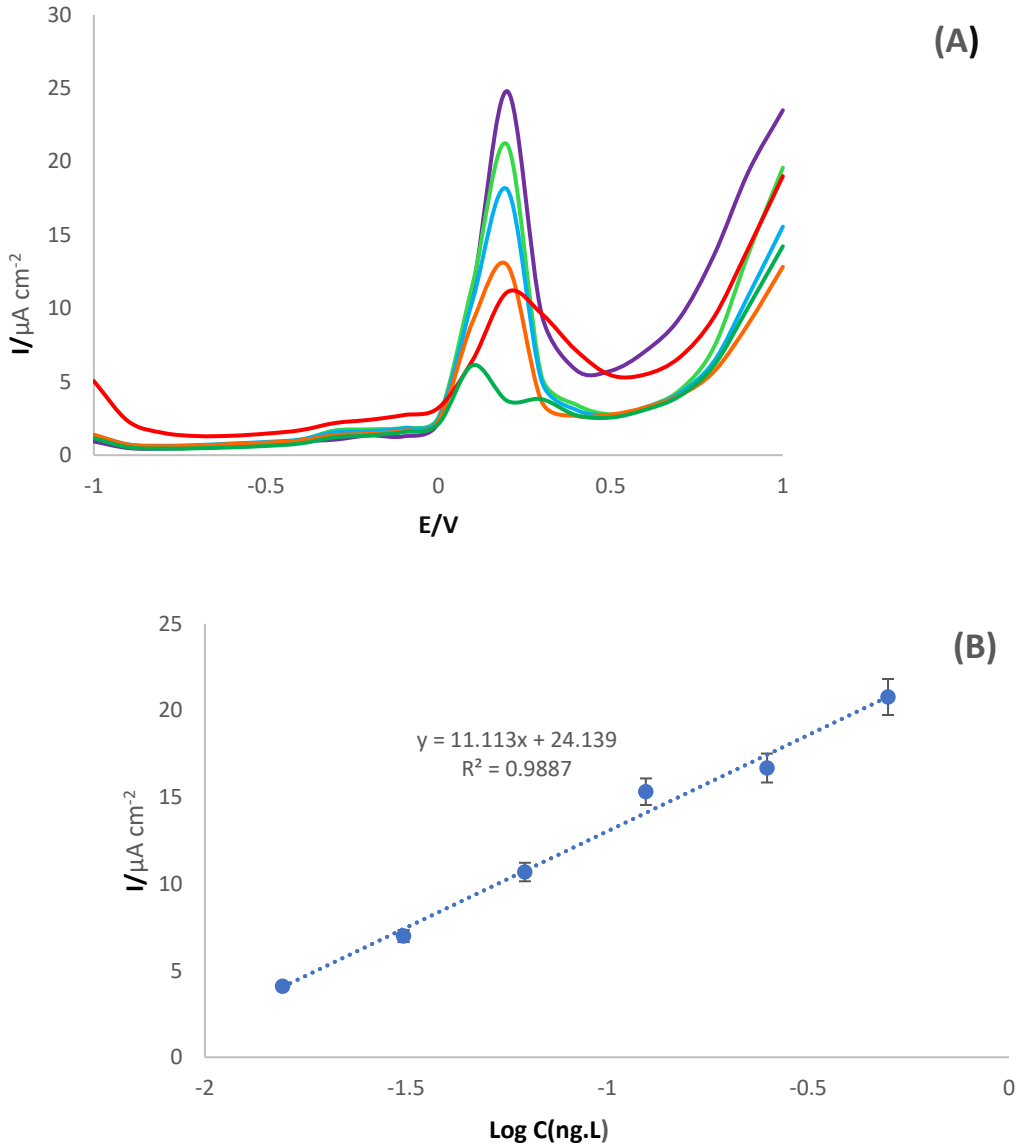

Figure S5. A) DPV responses of the immunosensor for different concentrations of 2-AG in human
plasma sample: 0.5, 0.25, 0.125, 0.0625, 0.0312, 0.0156 ng/l in 0.03M ferro/ferricyanide. **B)** the calibrations curves. (n=3, Sd=1.23).

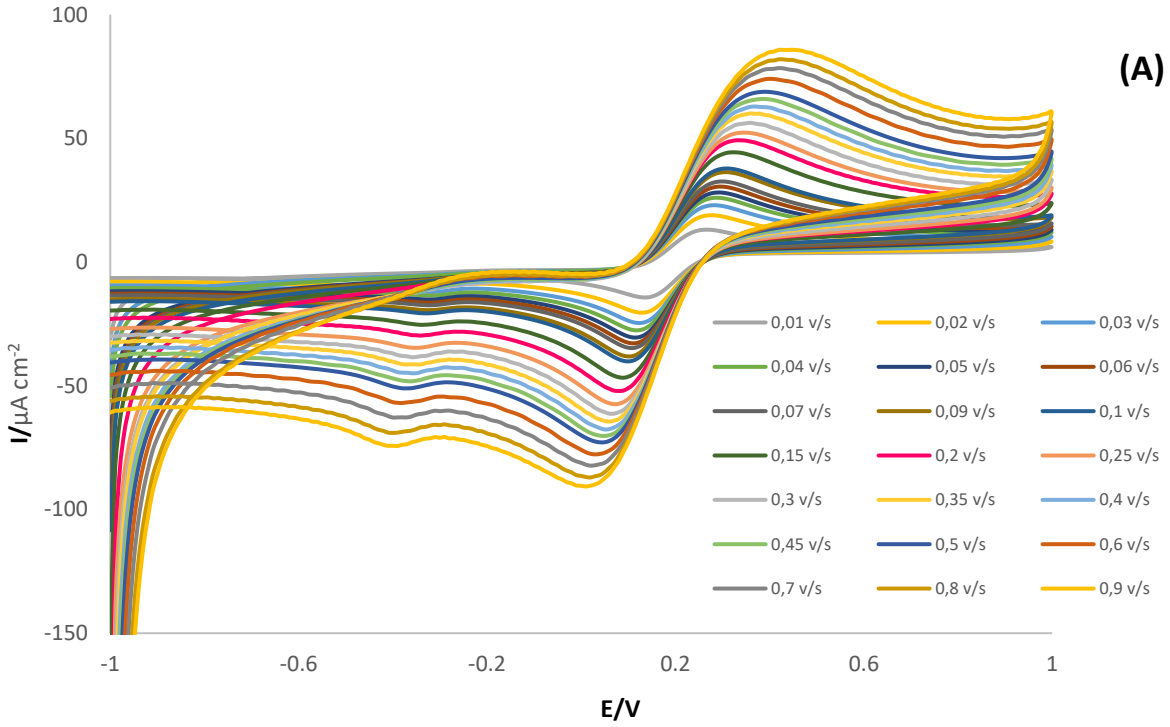
(A)
100
50
0
-50
-100
-150
-1
-0.6
-0.2
0.2
0.6
1
I/µA cm-2
E/V
0,01 v/s
0,02 v/s
0,03 v/s
0,04 v/s
0,05 v/s
0,06 v/s
0,07 v/s
0,09 v/s
0,1 v/s
0,15 v/s
0,2 v/s
0,25 v/s
0,3 v/s
0,35 v/s
0,4 v/s
0,45 v/s
0,5 v/s
0,6 v/s
0,7 v/s
0,8 v/s
0,9 v/s

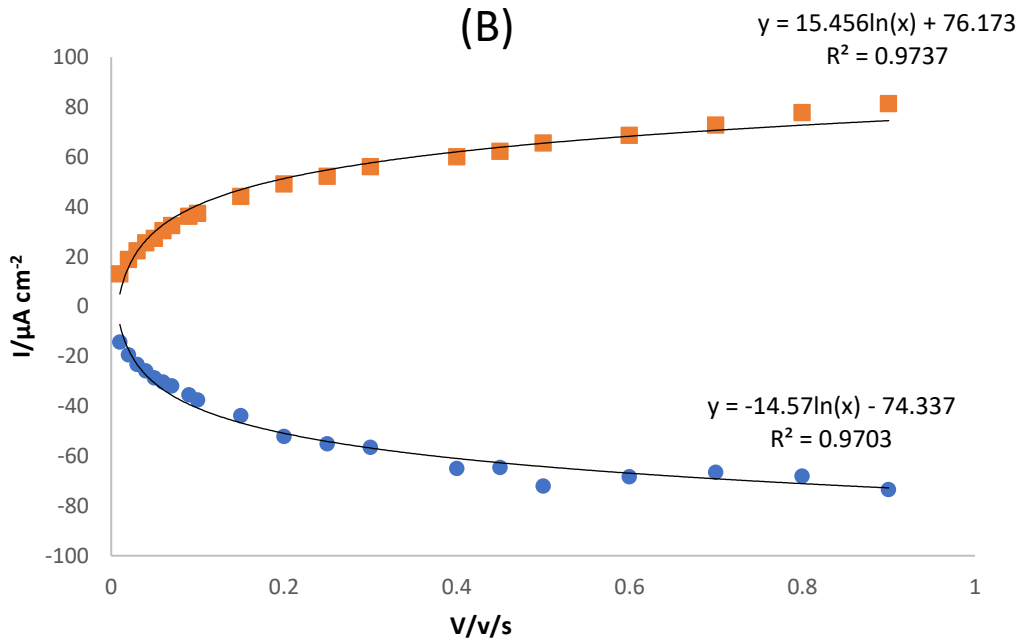
(B)
y = 15.456ln(x) + 76.173
R² = 0.9737
y = -14.57ln(x) - 74.337
R² = 0.9703
100
80
60
40
20
0
-20
-40
-60
-80
-100
0
0.2
0.4
0.6
0.8
1
I/µA cm-2
V/v/s

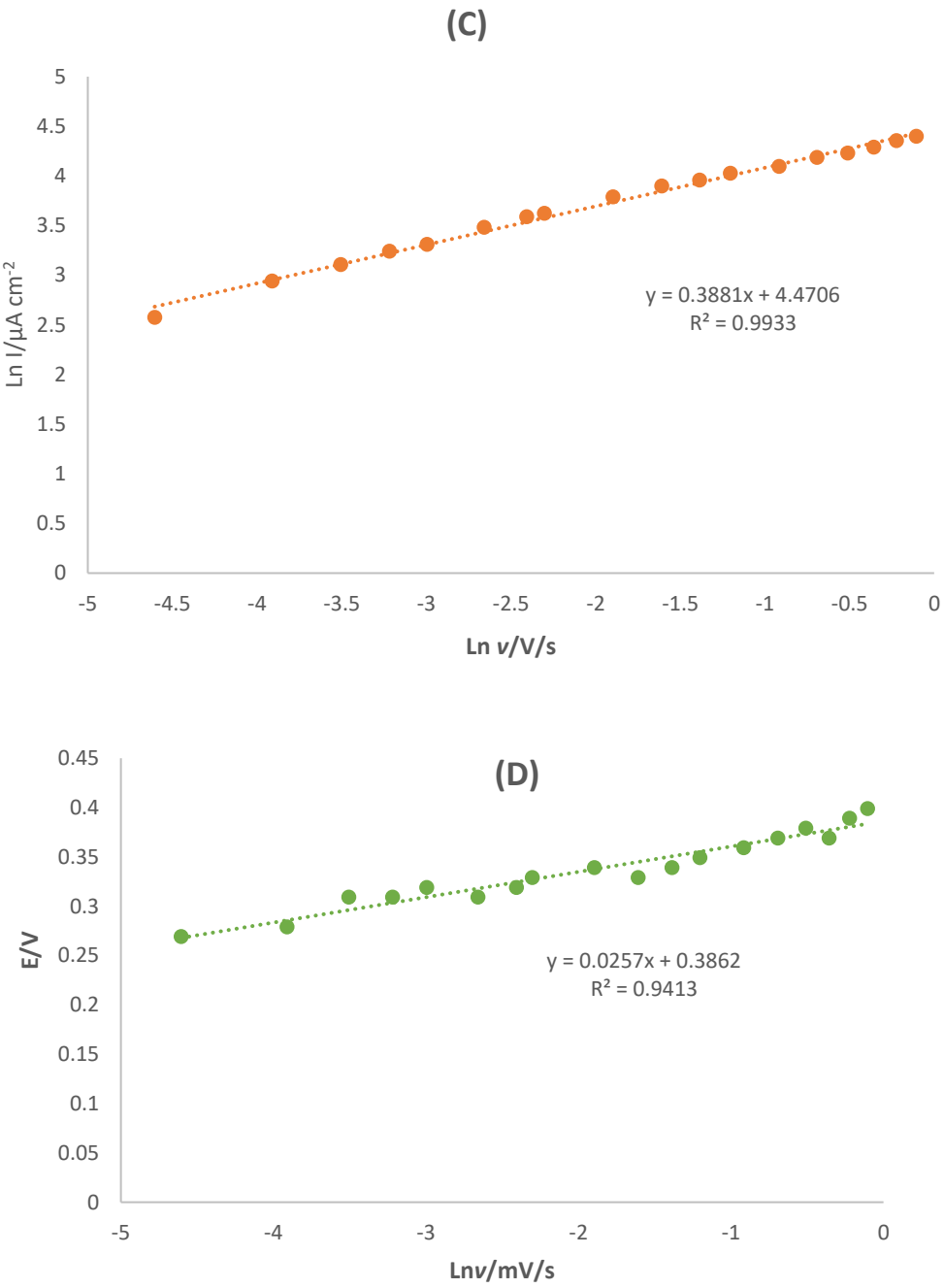

Figure S6. A) CVs of PβCD/GCE in the presence of 0.03M K_4 $Fe(CN)_6$/K_3 $Fe(CN)_6$/KCl in different potential scan rates (10–900 mV/s) **B)** Relationship between sweep rates and oxidation peak currents using CV technique. **C)** Relationship between the Neperian logarithm of peak current (ln I_{pa}) and Neperian logarithm of scan rate (ln *v*). D) Variation of peak potential versus Neperian logarithm of sweep rates.

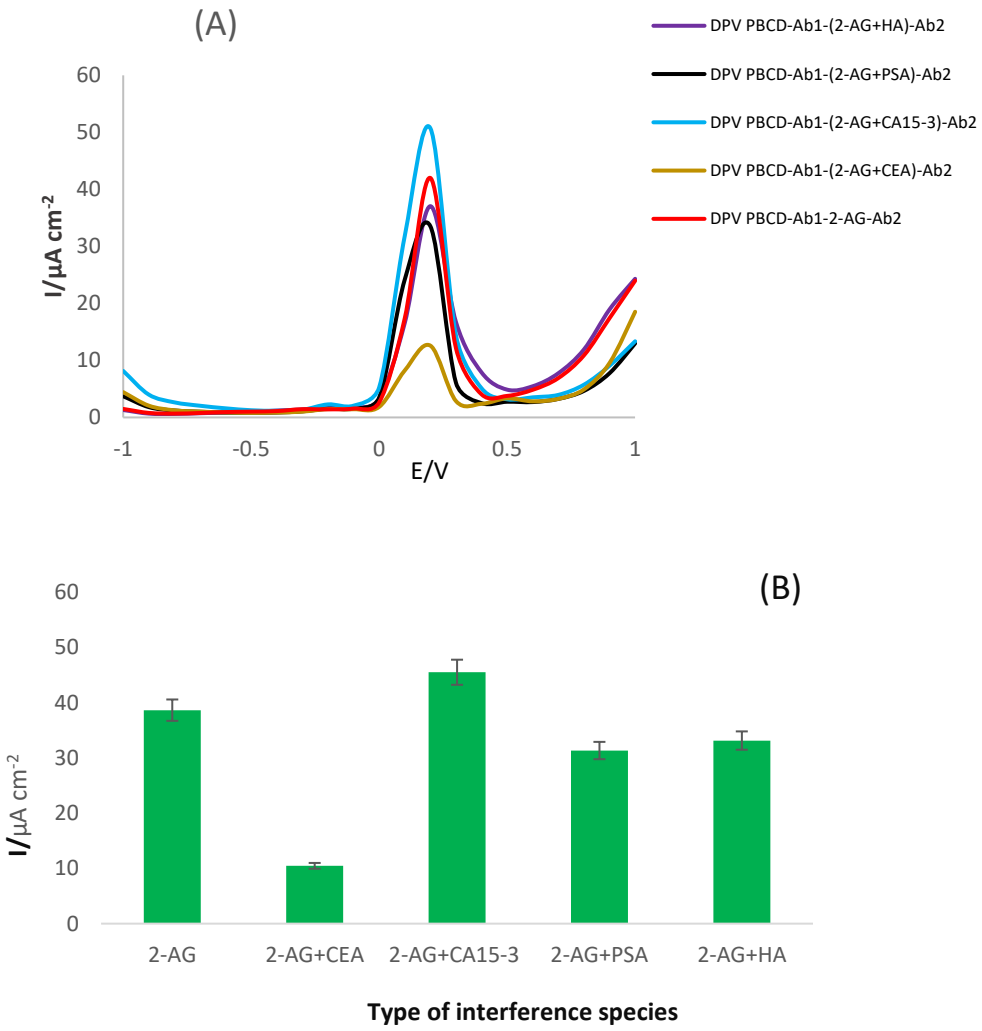

Figure S7. A) DPVs of the designed immunosensor in the presence of (CEA, CA15-3, PSA, HA) in
0.03 M K_4 $Fe(CN)_6$ /K_3 $Fe(CN)_6$/KCl in a potential range of -1 V to 1V at scan rate of 0.1 V/s. **B)** Histogram of peak currents *versus* the type of interfering agents (n=3, SD=1.95).

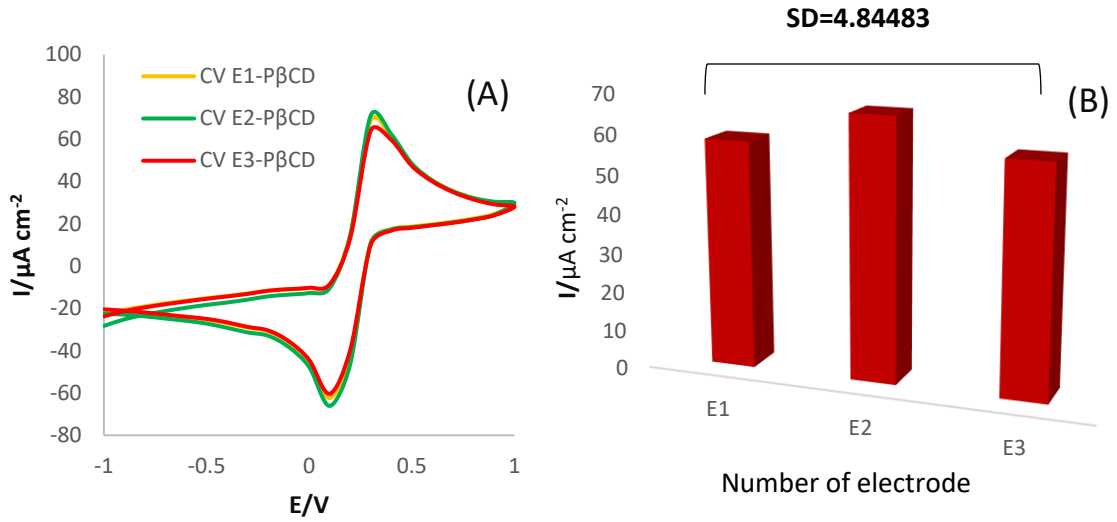

Figure S8. A) CVs of three p(β-CD)/GCE in the potential range of -1 to 1 in the solution of 0.03 M
$K_4Fe(CN)_6$ /K_3 $Fe(CN)_6$/KCl. **B)** Histogram of peak currents *vs.* the number of electrodes.

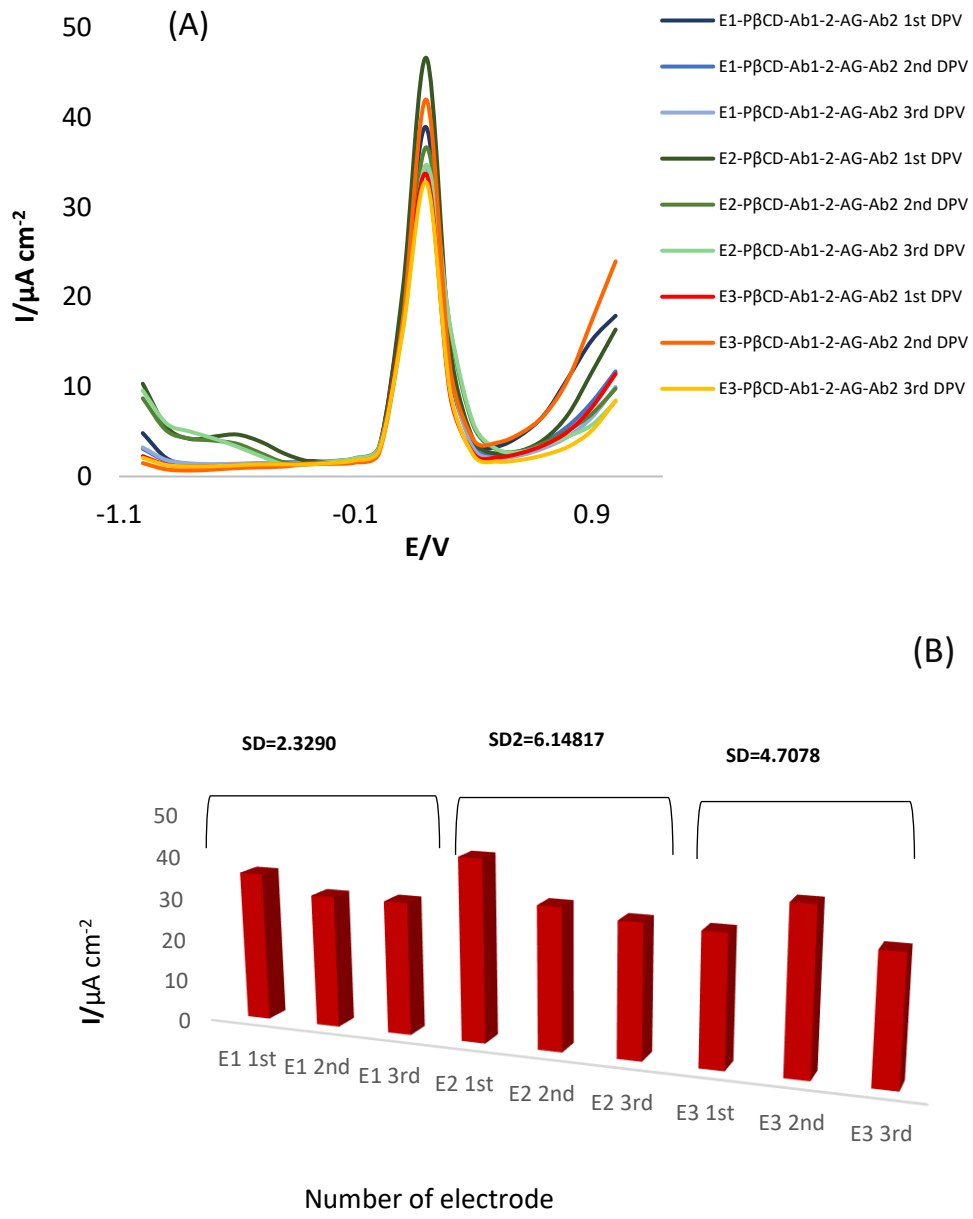

Figure S9. A) The DPVs of engineered immunosensor by three similar electrodes in the same condition. **B)** Histogram pf peak current versus number of electrodes. Potential range of -1 to +1 V at a scan rate of 0.1 V/s.

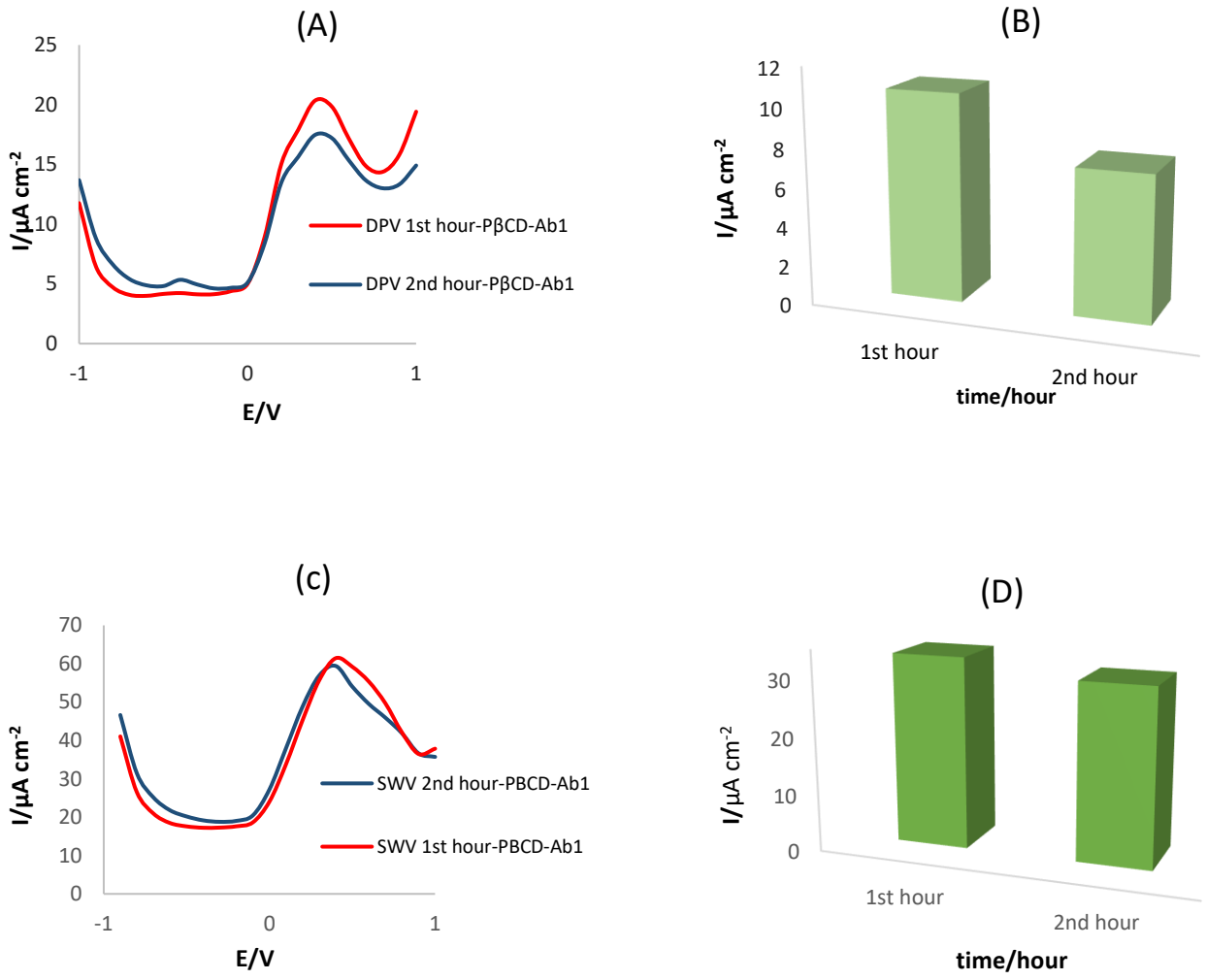

Figure S10. A) DPVs of P(βCD) /Ab1 modified GCE at different time of test. **B)** Histogram of peak current *versus* storage time of test (n=3, SD=1.29). **A)** SWVs of P(βCD) /Ab1 modified GCE at different time of test. **B)** Histogram of peak current *versus* time of test (n=3, SD=2.04).

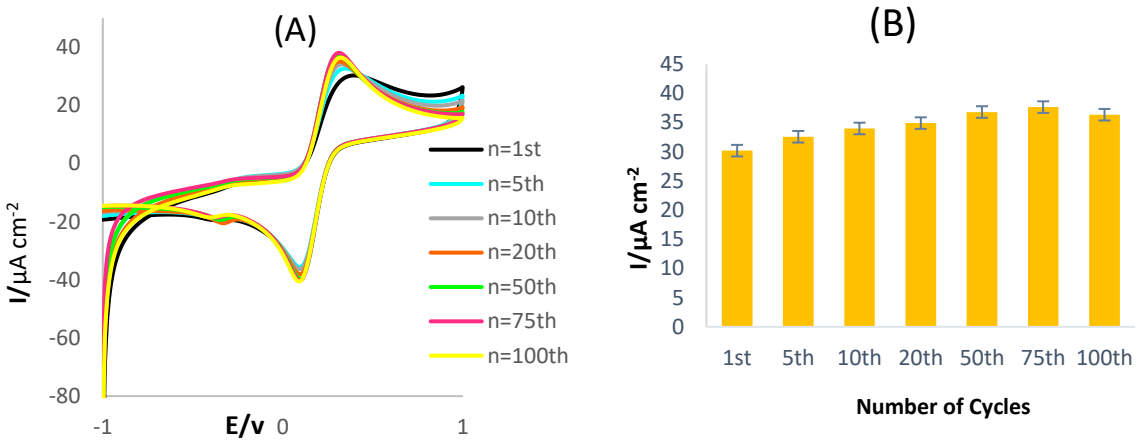

Figure S11. A) CV of P(β-CD)-GCE (polymeric interface) in the potential range of1 to 1 and scan rate of 0.1 V/s in 0.03M of ferro/ferricyanide in different cycle numbers. **B)** Histogram of peak current *vs* number of cycles (n=3, SD=1.55).

Table S1. Developed analytical methods for detection of 2-AG.

Detection methods	Type of Sample	LOD, LOQ, or LLOQ [a]	Linear range	Limitation/advantages	Ref.
HPLC-MS/MS	Plasma	8.0 ng/mL (LOD)	0.04-10.00 ng mL^{-1}	Expensive, hard to operation	[14]
LC-MS/MS		2 ng mL^{-1} (LOD)	-	Need for advanced tools	[15]
ELISA	Human adipose tissue	5 µM/L(LOD)	5 - 100 µM/L	Expensive, need for advanced process	[16]
LC-MS/MS	Plasma	190 ng mL^{-1} (LOQ)	0.04 - 12.3 ng mL^{-1}	Need for advanced tools	[17]
	Mouse brain	65 fmol (LOQ)	0.02–20 ng mL^{-1}	Expensive, need for expert personal	[18]
Electrochemical immunosensing	Biological	0.00024 ng L^{-1}(LOD)	0.00024–0.0078 ng L^{-1}	Easley and fast operation, no need for advanced tools	[19]
LC-MS/MS	Human cells	1.7 ng mL^{-1} (LOD)	-	Hard to operation, need to expert operator	[20]
Sandwich type electrochemical immunosensing	Human plasma	0.0078 ng/L (LLOQ)	0.0078 - 1.0 ng L	Relatively cheap, easy to operate, fast response	This Study

[a] **LOD**; Limit of detection, **LOQ**; Limit of quantification, **LLOQ**; Low limit of quantification